Towards Automating Tunnel Inspections with Optical Remote Sensing Techniques

Entwicklungen in Richtung automatisierter Tunnelinspektionen mit berührungslosen, optischen Messmethoden

Valentin Vierhub-Lorenz, Christoph S. Werner, Philipp von Olshausen, Alexander Reiterer

In this article a new concept and measurement results of a novel system that aims to replace the manual hammering for acoustic delamination detection using a remote sensing approach is presented. A strong, pulsed laser serves as a hammer and creates a plasma induced shockwave on the concrete surface. This shockwave excites characteristic, resonant vibrations if a delamination is present. A second laser is used to remotely detect these vibrations via a coherent measurement technique. In combination with a recently developed laser scanner, which allows the simultaneous measurement of the 3D-geometry and the detection of water on the tunnel surface via a multispectral approach, this novel system meets many requirements of tunnel inspections.

Keywords: Inspection, defect detection, instrumentation, remote sensing, building information modeling (BIM).

Im vorliegenden Beitrag werden ein neuartiges Konzept und erste Messergebnisse zu einem berührungslosen, optischen Messsystem präsentiert, das den manuellen Hammerschlagstest zur akustischen Detektion von Delaminationen ersetzen kann. Ein starker gepulster Laser dient als Hammerschlag, indem er eine plasmainduzierte Schockwelle auf der Betonoberfläche erzeugt. Bei Anwesenheit einer Delamination regt die Schockwelle charakteristische resonante Schwingungen der Oberfläche an. Die Vibrationen werden mit einem zweiten Laser mittels einer kohärenten Messmethode detektiert. In Kombination mit einem multispektralen Laserscanner, der darauf ausgelegt ist, gleichzeitig die hochaufgelöste Erfassung der 3D-Geometrie und die Detektion von Wasser auf der Tunneloberfläche zu ermöglichen, können viele Anforderungen von Tunnelinspektionen abgedeckt werden.

Schlüsselwörter: Tunnelinspektion, Fehlstellendetektion, Messgeräte, Remote Sensing, Building Information Modeling (BIM)

1 INTRODUCTION

Inspections are a crucial part in the operation of Tunnel structures that have to be performed in regular intervals and need to comprise specific tasks as for example stated in the /DIN 1076:1999/. The inspection typically includes the detection of cracks, spalling and delamination as well as water intrusion and deformation of the tunnel geometry. These tasks are often still performed visually or with the use of tactile instruments. Most companies and institutes that perform tunnel inspections already employ mobile laser scanners for mapping of the tunnel surface. Often devices scanning perpendicular to the driving direction (referred to as profilers) with a high measurement rate are being used. On the resulting photorealistic images of the surface the damages are then visualized. The state of the art for the detection of defects behind the tunnel surface is still the use of a hammer to excite resonance vibrations and the human ear as sensor to detect them. The results are time consuming manual labour, costly tunnel closures and subjective results.

With the increasing demand for Building Information Modeling (BIM) compliant data an automated process with an objective defect detection would be desirable. Two sensor systems that contribute towards this goal are presented. The first sensor combines surface moisture detection with high resolution laser scanning and has already entered the productive stage. The second sensor system aims to replace the manual hammering method for the detection of defects behind the tunnel surface by a remote sensing technique. The concept, our lab setup, and first measurement results from the lab are presented.

2 MULTISPECTRAL LASER SCANNER FOR SIMULTANEOUS MEASUREMENT OF THE 3D-GEOMETRY AND DETECTION OF WATER

2.1 Concept

We present a novel type of profile laser scanner designed for the automation of tunnel inspections. The goal of the scanner is to get fast, lighting independent, high resolution data of the tunnel surface by simultaneous measurements of the remission, distance, and surface moisture. To achieve this the measurement technique of an amplitude modulated phase measurement laser scanner is combined with the usage of two different laser wavelengths to create a multispectral laser scanner including a differential absorption measurement. The concept of multispectral laser scanning to gain additional information about the scanned surface has been reported many times. For example, /Gaulton et al. 2013/ showed that dual wavelength laser scanning with a 1 063 nm and 1 545 nm wavelength laser can be used to estimate water content in vegetation. Most multispectral laser scanners are based on pulsed time of flight method and compare the reflectivity of one wavelength in the visible region with one in the near infrared region for example for vegetation monitoring /Li et al. 2018/. The pulsed method makes it difficult to compare the backscattered signal strengths of the individual lasers since they usually don't synchronously illuminate the same surface. In the following section the concept and technical realisation of our multispectral scanner based on amplitude modulation will be described briefly. The working principle and a proof of concept have been presented in more detail before /Vierhub-Lorenz et al. 2019/. The absorption coefficient of liquid water for the near infrared region can be seen in *Fig. 1*. Two distinct absorption bands at approximately 1 450 nm and 1 920 nm are present. Due to the availability of suitable laser sources the absorption band at 1 450 nm wavelength was chosen for the differential absorption. The reference wavelength was set to 1 320 nm to be as close as possible to the first wavelength without being affected by the absorption band. This ensures that achromatic aberrations caused by the collectively used optics are kept as small as possible. The backscattered intensities of a surface illuminated by the two lasers are compared and a moisture value M similar to the normalized difference vegetation index (NDVI) is calculated using the formula:

$$M = \frac{I_{1320} - I_{1450}}{I_{1320}}, \tag{1}$$

where I_{1320} denotes the backscattered intensity at the reference wavelength of 1 320 nm and I_{1450} the backscattered intensity at the absorption band at a wavelength of 1 450 nm. Both intensities are normalized to the backscattered intensity of a reference target with approximately 90 % reflectivity at both wavelengths.

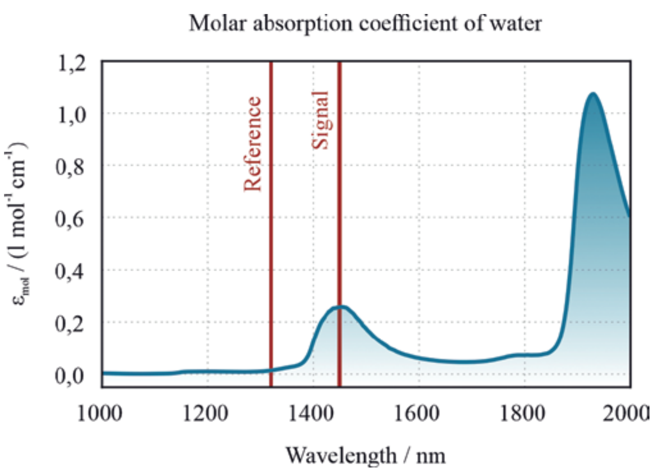

Fig. 1 | Graph of the literature values for the molar absorption coefficient of water in the near infrared region as reported by /Bertie & Lan 1996/. The wavelengths of 1 320 nm and 1 450 nm used in the laser scanner for the detection of water are indicated.

2.2 Technical Realisation

The combination of distance measurement and the detection of water is done by modulating the amplitudes of the two fiber coupled lasers with different frequencies. The laser light is then combined into one single mode fiber before being collimated to a beam. The beam is then deflected by a rotating 45° mirror along a circular scan line of 350°. The remaining 10° are blocked by a mounting part which is also used as a reference to compensate the distance measurement for drifts. The rotation speed of the mirror can be set up to 200 Hz. The backscattered light is collected and deflected by the same mirror and focused by the receiving optics onto a single photodetector.

The signal contributions of the two lasers are separated by filtering for their respective modulation frequency. For each frequency the amplitude, which corresponds to the backscattered intensity, and the phase compared to that of a local oscillator are determined. The phase difference $\Delta\theta$ and the modulation frequency f can be used to calculate the distance D to the surface using the speed of light c:

$$D = \frac{\Delta\theta\, c}{4\pi f} + \frac{n\, c}{2f}. \tag{2}$$

The second term, with the arbitrary integer n, defines the unambiguity range, because after one wavelength the phase repeats. Therefore, the measurement range is limited to half the wavelength of the lowest modulation frequency. An image of the laser scanner is shown in *Fig. 2*. The scanner performs

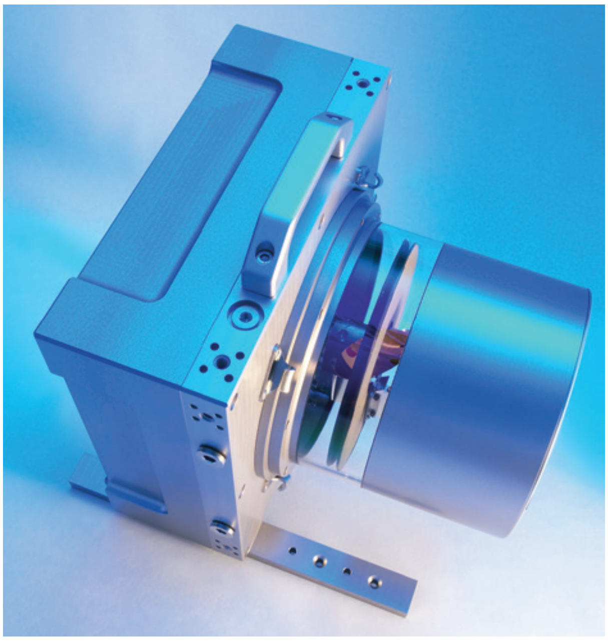

Fig. 2 | Photograph of the Tunnel Inspection System (TIS) with simultaneous distance, intensity, and moisture measurement /Fraunhofer IPM/

the phase and amplitude measurements, which result in a distance, intensity, and moisture measurement, with a rate of 2 MHz. The standard deviation of the distance measurement is approximately 2 mm on a target with 90 % reflectivity in 10 m distance. The distance measurement error due to nonlinearities is also about 2 mm for the measurement range from 1 m to 10 m. The footprint of the laser in 10 m distance is approximately 8 mm. The Moisture Value can take values from –1 to 1. Most dry materials reflect both wavelengths equally resulting in a Moisture Value around 0. Wet objects with excess water on the surface or water containing objects like plants usually show Moisture Values around 0.5 which means that the light at 1 450 nm wavelength gets absorbed 50 % stronger than the light at 1 320 nm wavelength. The standard deviation of the Moisture Value for a dry target with 90 % reflectivity at a distance of 5 m is approximately 0.05.

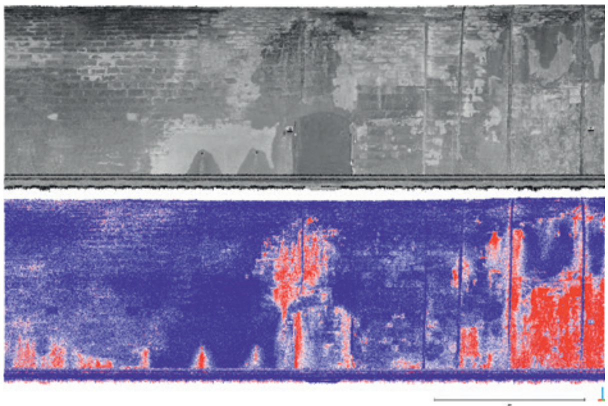

Fig. 3 | Top: Greyscale intensity image of a point cloud section of a rail tunnel. Bottom: Same tunnel section colored using the moisture value. The color scale goes from blue ($M = 0$) for dry surfaces over white to red ($M = 0.5$) for wet surfaces.

2.3 Field Tests

In cooperation with Amberg Technologies the laser scanner was tested under real conditions in a railway tunnel. The measurements were performed with the scanner mounted on one of Amberg Technologies rail-based mobile mapping systems. A section of the resulting point cloud of the tunnel in intensity-based greyscale as well as coloured using the moisture value is visualized in *Fig. 3*. In the intensity-based greyscale image the details of the tunnel surface are visible. Areas of different reflectivity are well visible. Darker areas often correspond to water on the tunnel surface but, especially for older tunnels, due to contaminations on the surface the intensity alone can be misleading. The additional information of the moisture channel clearly shows the wet areas and can potentially be used for their automated detection.

3 DETECTION OF NON-VISIBLE DEFECTS BY A LASER BASED SENSOR SYSTEM

3.1 Concept

A more difficult task is the detection of damages behind the tunnel lining that are not visible. Here the goal is to imitate the principle of the current state of the art, the hammering method, with a remote sensing technique. A strong, pulsed laser is used to create a plasma induced shock wave on the concrete surface, substituting the manual hammering. The shock wave will, if cavities or defects are present, excite resonance vibrations whose amplitudes and frequencies depends on the size and depth of the cavities and defects. Typical defects in tunnel structures that can be detected with the hammering method show resonance frequencies from few 100 Hz up to around 10 kHz. In the classical hammering approach these resonance vibrations are detected by the resulting acoustic waves by the inspection personal. In the remote approach a laser doppler vibrometer (LDV) directly measures the movement of the concrete surface via the doppler shift of the backscattered light. Generating ultrasound signals in a material via laser illumination and measuring them via interferometric measurement methods is used for various applications in material research such as inspection of polymer composites, microelectronic components or thickness measurements of steel tubes /Jean-Pierre Monchalin 2004/. These applications all have a small measurement distance of below 1 m in common. /Algernon 2006/ could show the possibility to detect flaws in concrete via measurement of ultrasound signals with an LDV but here the sound waves were excited by mechanical impact. Apart from the countless applications and findings on laser-based ultrasound measurements, research has also been done on the detection of resonance vibrations originating from defects in concrete via laser doppler vibrometers. /Masayasu Muramatsu et al. 2020/ detected flaws in concrete via LDV measurements from a commercial device by exciting resonance vibrations with the impact of a hammer. To achieve fully non-contact measurements /Kazuko Sugimoto et al. 2019/ presented their results on exciting resonance vibrations of defective concrete areas with sound waves from a long-range acoustic device and measuring them successfully with a commercial scanning LDV. The downside of their approach is the relatively low measurement rate of less than one per second that is mainly caused by the time needed to excite the resonance vibrations with sound. /Kurahashi et al. 2018/ presented successful measurements of resonance vibrations with a two-wave-mixing interferometer that were excited using a pulsed nanosecond laser with high pulse energy. This method would allow for fast, non-contact measurements of excited resonance vibrations over several meters distance. But still there remain many unanswered questions about this topic that require further research and so far there are no commercially available systems for tunnel inspections based on the working principle of laser excitation and measurement of resonance vibrations.

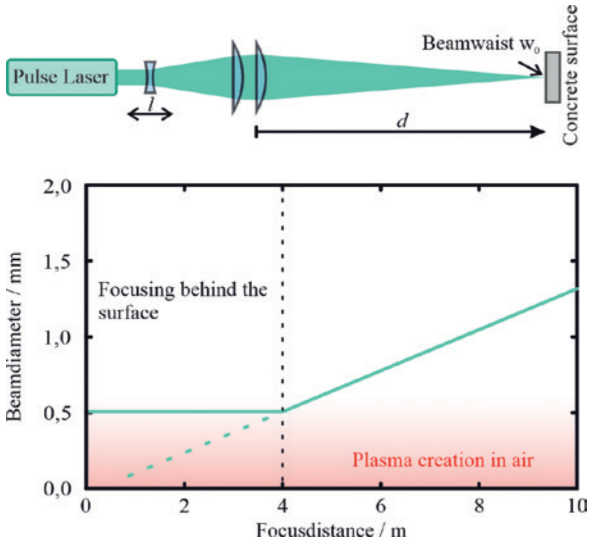

Fig. 4 | Top: Schematic depiction of the setup used for the excitation of resonance vibrations by creation of a plasma on the target surface. Bottom: Theoretical achievable spot diameter of the setup for a gaussian beam. Below 4 m distance the laser is focused behind the surface to avoid the accidental creation of plasma in air.

3.2 Technical Realisation

For the impact laser a Spectra Physics Quanta Ray PRO 250-10H with up to 1 J pulse energy, 20 ns pulse duration and 10 Hz repetition rate is used, which is limiting the maximum measurement rate. A biconcave lens with 50 mm focal length and a lens pair with 500 mm focal length each are used as a beam expander. The exit diameter of the laser is about 5 cm. By adjusting the position of the small lens l between 250 ± 50 mm, the focus distance d can be adjusted from approximately 1 m to 10 m. A schematic depiction can be seen in *Fig. 4*. In the lab setup the beam is deflected by a mirror (not shown) which can manually be tilted to scan a surface on a test specimen. Focusing the beam on the concrete surface leads to the creation of a plasma and therefore a shockwave that can excite resonance vibrations. Increasing the laser beam diameter at the exit aperture of the system is necessary to achieve a small focus spot on surfaces that are further away. On the other hand, the spot diameter should not be too small to avoid the accidental creation of a plasma in air before the pulse reaches the target surface. /Tambay et al. 1991/ and /Thiyagarajan & Thompson 2012/ found that plasma in air at atmospheric pressure is generated when the intensity surpasses approximately $5 \cdot 10^{11}$ W/cm^2. For the parameters of our laser this results in a minimum spot diameter of 55 µm. In our experiments even with a spot diameter of approximately 250 µm a plasma in air could still be observed. For a spot diameter over 0.5 mm a plasma occurred only rarely. The fluctuations are probably a result of impurities, e. g. dust particles in the air that absorb the light much stronger. The theoretical minimum spot diameter for a gaussian beam with our setup is plotted in *Fig. 4*. For distances closer than 4 m the focus is set behind the surface so the spot diameter on the surface stays at 0.5 mm and an accidental creation of plasma in the air is avoided.

For the detection of the excited resonance vibrations, we are building our own laser doppler vibrometer (LDV). This way we can optimize it for our use case scenario and measurement conditions. *Fig. 5* shows a schematic depiction of the setup of the LDV. The crucial component of the LDV is an ultra-narrowband Koheras Basik X15 fiber laser with a linewidth < 100 Hz and a wavelength of 1 550 nm. The power is split into a local oscillator (LO) and a signal channel. The frequency of the signal beam is shifted by an acousto-optic modulator by 40 MHz to obtain a heterodyne signal. It is then amplified by an erbium doped fiber amplifier (EDFA) and again split into a measurement and reference channel. The measurement channel with an optical power of approximately 200 mW passes through a polarisation beam splitter (PBS) and is then focused by a lens with 60 mm focal length onto the surface. The backscattered light from the surface is collected by the same lens. Due to the roughness of the surface the backscattered light is mostly depolarized so half of it is transmitted back by the PBS towards the exit fiber but the other half is reflected into the signal fiber. The backscattered light is then mixed with the LO in a 50/50 beam splitter and coupled onto a balanced photodetector. The resulting electrical beat signal is digitized by an analog-to-digital converter (ADC) with a sampling rate of 250 Msps and evaluated by

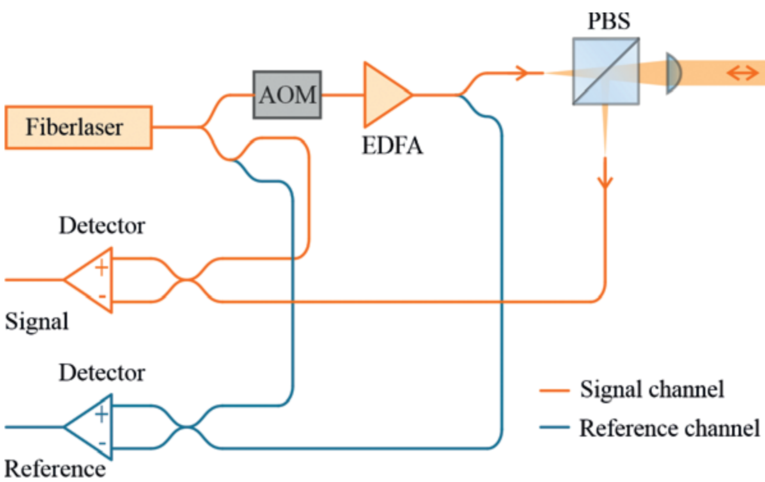

Fig. 5 | Schematic depiction of the laser doppler vibrometer setup results an FM demodulation algorithm on a computer, that transforms the doppler shift frequency into displacement information. The signals are bandpass filtered and decimated to match our application specific frequency range of 500 Hz to 15 kHz. The signal of the reference channel is subtracted from the signal channel to filter noise induced by the laser and other components of the LDV.

3.3 Results

A concrete block with a size of 80 cm × 80 cm × 80 cm containing artificial defects of different sizes in a depth of approximately 3 cm is used as a test object. The defects were induced by embedding a sheet of extruded polystyrene foam below the concrete surface to imitate a delamination. A photograph of the concrete block can be seen in *Fig. 6*. Four positions are marked where measurements have been performed. Positions 1 to 3 mark the center of defects with a size of 20 cm × 20 cm, 16 cm × 16 cm and 12 cm × 12 cm, respectively. Position 4 is an intact surface. The first two defects are easily detectable using manual hammering and the human ear as the detection sensor, the third one is barely detectable. For the measurements the concrete block was placed approximately 2 m in front of the measurement setup and the LDV was focused on the marked spots. The excitation laser was focused 2 cm below the measurement spot. An exemplary measurement signal of the displacement is shown in *Fig. 7*. After the laser pulse hits the surface at around 8 ms, a decaying oscillation is clearly visible. A Fourier transformation of the time frame marked in green is performed and the resulting spectra are normed to the amplitude at position 1. The analyzed time window is chosen to start shortly after the shock wave of the laser pulse and ending ~7 ms later, before the background noise induced by the shockwave sets in. The resulting spectra for the 4 measurement positions are also shown in *Fig. 7*. All spectra show a small peak around 500 Hz which is a result of low frequency background noise. The frequency spectra of all three defects show pronounced peaks. The amplitude is lower for smaller defect size while the frequencies go up. For position 1 a prominent resonance frequency around 1.8 kHz and a smaller one at 3.5 kHz can be seen. Position 2 show two resonance frequencies separated by approximately 500 Hz around 3 kHz and position 3 shows two also separated by 500 Hz around 5 kHz. Position 4, where no defect is present, shows no pronounced resonance frequencies.

Further the dependency of the resonance amplitude on the pulse energy was investigated. /Mikami et al. 2020/ suggest that the spectral power in the resonance frequencies scales linear with the pulse energy in the region from 20 to 300 mJ for a spot diameter of

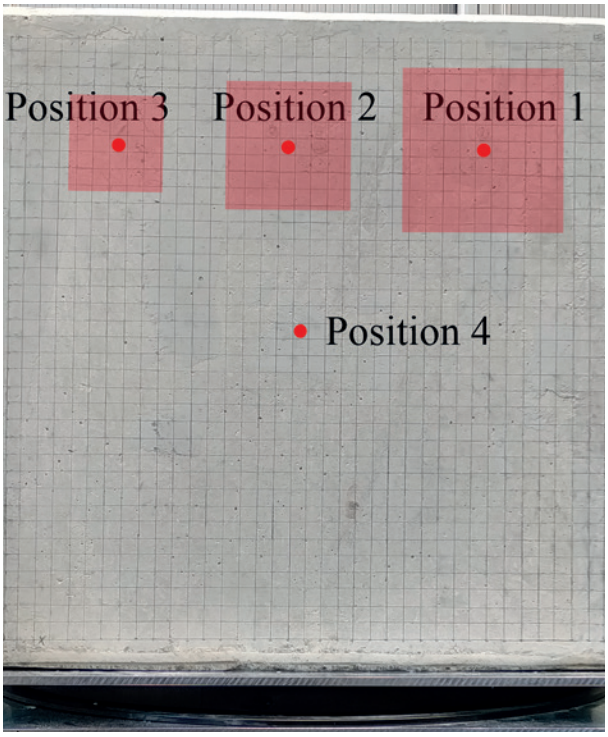

Fig. 6 | Photograph of the concrete block with artificial defects used for test measurements in the lab. The three defect areas are indicated and the measurement positions are marked by red dots

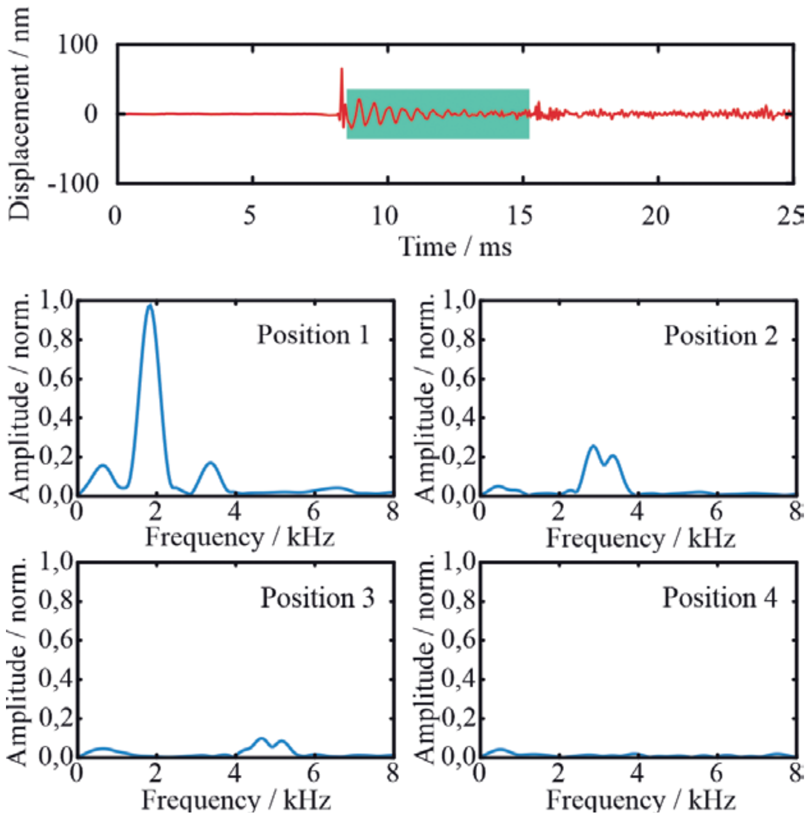

Fig. 7 | Top: Displacement measured by the LDV on position 1. The laser pulse hits the surface at around 8 ms. The resonance vibration is clearly visible in the region highlighted in green. Bottom: Resulting frequency spectra of the resonance vibrations.

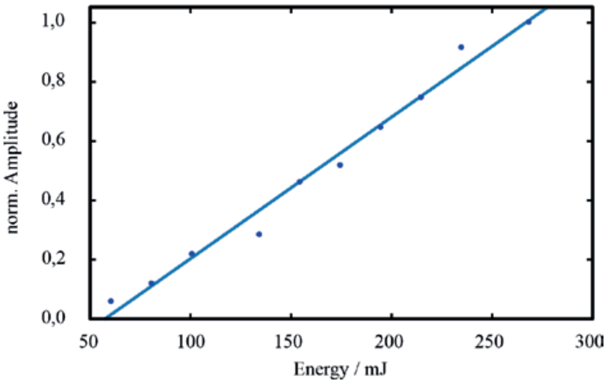

Fig. 8 | Measured resonance vibration amplitude for pulse energies from 55 mJ to 270 mJ with a linear fit

0.5 mm and a 10 ns pulse duration. The results of our experiments in the range from 55 to 270 mJ with a spot diameter of approximately 350 µm in 2 m distance can be seen in *Fig. 8*. The resonance frequency amplitudes were measured with our LDV and normed to the value at 270 mJ while the pulse energies were measured using a Thorlabs ES245C Powermeter. The results confirm the linear dependency of the resonance amplitude with the pulse energy in this intensity regime.

Our first measurements show that it is possible to excite resonance vibrations in concrete surfaces using a laser induced plasma and detect them using an LDV. We could show that it is possible to distinguish between defects of different sizes and areas without defects by analyzing the frequency spectra. In our future work we will continue finding the ideal parameters for the laser-based excitation of resonance vibrations and optimizing the LDV. We will especially focus on developing a motorized scanning and focusing system and making the measurement system robust and reliable for measurements outside the lab environment under real conditions. A major task here will be the suppression and filtering of ambient vibrations on the system or the surface.

4 CONCLUSION

We presented two sensor systems that can contribute to the automation of tunnel inspections in the near future and deliver BIM compliant data. The TIS provides a high-resolution 3D-model of the Tunnel that can be coloured using regular intensity values or the moisture value. To our knowledge this combination of wavelengths together with a high measurement rate, scanning speed and accuracy are unique and make the system a perfect tool for tunnel inspections. Its data could be used to detect deformations and defects on the surface like spalling and water intrusion automatically. The high popularity and fast paced development in the field of artificial neural networks (ANN) makes them promising candidates for automated defect detection. Some promising results regarding the automatic detection of spalling using ANN on laser scanning data have for example already been presented by /Zhou et al. 2021/ but also many other inspection companies are starting to implement ANN-based defect detection. For the detection of water intrusion on the other hand a simpler algorithm, for example using a threshold on the moisture value combined with a minimum surface area, could already be sufficient.

For the second sensor system we presented our concept and the current status of the lab setup. We could show that it is possible to remotely excite and measure resonance vibrations in concrete structures with our laser-based sensor system. We presented the resulting spectra of different defect sizes and an intact surface that can clearly be distinguished. A distinction between a healthy surface and a defect below the surface is therefore generally possible. We could provide data and results, such as the expected frequencies and amplitudes of typical delaminations close to the concrete surface, that can hopefully contribute to the development of an automated measurement system combining an LDV and pulsed laser with fast and precise beam deflection and focusing units tailored to the application of delamination detection on concrete linings.

The automatic interpretation of the data generated by the measurement system is another field of research. Without large sets of real-world data and due to the variety of different tunnel types the usage of regular ANN is difficult. A promising approach is the use of clustering algorithms that don't need training data to find anomalies in the vibration spectra of a tunnel surface as presented by /Heinze et al. 2021/.

After confirming the working principle and collecting application specific experience, the focus now lies on the development of a robust scanning system that works under real conditions. This will require further research into the possibilities of fast scanning methods and also the effects of environmental influences such as ambient noise or contamination e.g. dust. The overall goal is to use the system on a mobile platform together with the TIS and a positioning unit. This will allow to fuse the data of the two systems to visualize the defects directly in the georeferenced 3D-model of the tunnel which could then be used for BIM compliant monitoring.

5 ACKNOWLEDGEMENTS

We would like to give special thanks to our colleagues and project partners Michael Geist, Christoph Heinze and Karsten Weiher from Fraunhofer IGP for their constructive feedback and the designing and manufacturing of the concrete block used for our test measurements in the joint research project "LaserBeat" financed by Fraunhofer-Gesellschaft.

We also want to thank our project partners Amberg Technologies for the joint test measurements in railway tunnels as part of the EuroStars research project "E!12267 OpOrTunIty".

REFERENCES

Algernon, D. (2006): Impact-Echo: Analyse akustischer Wellen in Beton. Doctoral Thesis. https://doi.org/10.14279/depositonce-1380.

Bertie, J. E.; Lan, Z. (1996): Infrared intensities of liquids XX: The intensity of the OH stretching band of liquid water revisited, and the best current values of the optical constants of H_2O(l) at 25°C between 15,000 and 1 cm^{-1}. In: Applied Spectroscopy 50(1996)8, 1047–1057.

DIN 1076:1999: Ingenieurbauwerke im Zuge von Straßen und Wegen: Überwachung und Prüfung. Ausgabe November 1999. Beuth, Berlin.

Fraunhofer IPM (2022): Objekt- und Formerfassung. https://www.ipm.fraunhofer.de/de/gf/objekterfassung-laserscanning.html (20.10.2022).

Gaulton, R.; Danson, F. M.; Ramirez, F. A.; Gunawan, O. (2013): The potential of dual-wavelength laser scanning for estimating vegetation moisture content. In: Remote Sensing of Environment 132(2013), 32–39. https://doi.org/10.14279/depositonce-138010.1016/j.rse.2013.01.001.

Heinze, C.; Vierhub-Lorenz, V.; Weiher, K.; Werner, C.; Geist, M. (2021): Automatisierte akustische Prüfung von Tunnelstrukturen mit Hilfe von Lasersystemen und maschinellem Lernen. DGZfP Jahrestagung (virtuell), Mai 2021. http://www.ndt.net/?id=26247.

Kurahashi, S.; Mikami, K.; Kitamura, T.; Hasegawa, N.; Okada, H.; Kondo, S.; Nishikino, M.; Kawachi, T.; Shimada, Y. (2018): Demonstration of 25-Hz-inspection-speed laser remote sensing for internal concrete defects. In: Journal of Applied Remote Sensing 12(2018)1, 015009. https://doi.org/10.1117/1.JRS.12.015009.

Li, Z.; Schaefer, M.; Strahler, A.; Schaaf, C.; Jupp, D. (2018): On the utilization of novel spectral laser scanning for three-dimensional classification of vegetation elements. In: Interface Focus 8(2018)2, 20170039. https://doi.org/10.1098/rsfs.2017.0039.

Mikami, K.; Hasegawa, N.; Kitamura, T.; Okada, H.; Kondo, S.; Nishikino, M. (2020): Characterization of laser-induced vibration on concrete surface toward highly efficient laser remote sensing. In: Japanese Journal of Applied Physics 59(2020)7, 76502. https://doi.org/10.35848/1347-4065/ab9849.

Monchalin, J.-P. (2004): Laser-Ultrasonics: From the Laboratory to Industry. In: AIP Conference Proceedings 700(2004)3, 3–31. https://doi.org/10.1063/1.1711602.

Muramatsu, M.; Uchida, S.; Takahashi, Y. (2020): Noncontact detection of concrete flaws by neural network classification of laser doppler vibrometer signals. In: Engineering Research Express 2(2020)2, 025017.

Sugimoto, K.; Sugimoto, T.; Utagawa, N.; Kuroda, C. (2018): Detection Effect of Resonance Frequency of Both Laser Doppler Vibrometer and Internal Defect of Concrete Structure by Spatial Spectral Entropy. In: 2018 IEEE International Ultrasonics Symposium (IUS), Kobe, Japan, 1–9. https://doi.org/10.1109/ULTSYM.2018.8580050.

Tambay, R.; Muthu, D. V. S.; Kumar, V.; Thareja, R. K. (1991): Laser induced air breakdown using 0.355, 0.532, and 1.06 µm radiation. In: Pramana 37(1991)2, 163–166.

Thiyagarajan, M.; Thompson, S. (2012): Optical breakdown threshold investigation of 1064 nm laser induced air plasmas. In: Journal of Applied Physics 111(2012), 073302. https://doi.org/10.1063/1.3699368.

Vierhub-Lorenz, V.; Predehl, K.; Wolf, S.; Werner, C.; Kühnemann, F.; Reiterer, A. (2019): A multispectral tunnel inspection system for simultaneous moisture and shape detection. In: Remote Sensing Technologies and Applications in Urban Environments IV. https://doi.org/10.1117/12.2533101.

Zhou, M.; Cheng, W.; Huang, H.; Chen, J. (2021): A Novel Approach to Automated 3D Spalling Defects Inspection in Railway Tunnel Linings Using Laser Intensity and Depth Information. In: Sensors 21(2021), 5725. https://doi.org/10.3390/s21175725.

AUTOREN

Valentin Vierhub-Lorenz

FRAUNHOFER INSTITUT FÜR PHYSIKALISCHE MESSTECHNIK IPM

Georges-Köhler-Allee 301 | 79110 Freiburg | Germany
valentin.vierhub-lorenz@ipm.fraunhofer.de |
ORCID: 0000-0002-9887-9337

Dr. Christoph Werner

FRAUNHOFER INSTITUT FÜR PHYSIKALISCHE MESSTECHNIK IPM

Georges-Köhler-Allee 301 | 79110 Freiburg | Germany
www.ipm.fraunhofer.de | christoph.werner@ipm.fraunhofer.de

Dr. Philipp von Olshausen

FRAUNHOFER INSTITUT FÜR PHYSIKALISCHE MESSTECHNIK IPM

Georges-Köhler-Allee 301 | 79110 Freiburg | Germany
www.ipm.fraunhofer.de | philipp.olshausen@ipm.fraunhofer.de

Prof. Dr. Alexander Reiterer

FRAUNHOFER INSTITUT FÜR PHYSIKALISCHE MESSTECHNIK IPM

ALBERT-LUDWIGS-UNIVERSITÄT FREIBURG – INSTITUT FÜR NACHHALTIGE TECHNISCHE SYSTEME INATECH

Georges-Köhler-Allee 301 | 79110 Freiburg | Germany |
www.ipm.fraunhofer.de | alexander.reiterer@ipm.fraunhofer.de

Emmy-Noether-Straße 2 | 79110 Freiburg | Germany | www.inatech.de
ORCID: 0000-0002-3196-3876